

# THE USE OF ORANGE-RED EMITTING $Ba_2Ca(BO_3)_2 : Sm^{3+}$ PHOSPHOR TO IMPROVE CHROMATICITY AND LUMINANCE OF CONVENTIONAL WHITE LEDS

Nguyen Thi Phuong Thao<sup>1</sup>, Hsiao-Yi Lee<sup>2,\*</sup>

<sup>1</sup>Faculty of Electrical and Electronics Engineering, Ton Duc Thang University, Ho Chi Minh City, Vietnam.

<sup>2</sup>Department of Electrical Engineering, National Kaohsiung University of Science and Technology, Kaohsiung, Taiwan.

\*Corresponding Author: Hsiao-Yi Lee (leehy@nkust.edu.tw)

(Received: 31-October-2024; accepted: 06-March-2025; published: 31-March-2025)

<http://dx.doi.org/10.55579/jaec.202591.475>

**Abstract.** The characteristics of configuration and illumination of  $Sm^{3+}$  incorporated  $Ba_2Ca(BO_3)_2$  samples produced using the traditional solid-status approach are discussed in this study. The luminescence measurement of the prepared red phosphor and phosphor-conversion sheet for white light emitting diodes (WLED) were conducted with Mie-scattering Monte Carlo simulation and MATLAB computation. The phosphor demonstrated a broad emission range with the prominent emission peak at 601 nm under the 402 nm radiation, originated from the  $Sm^{3+}$  ion's  $^4G_{5/2}$  and  $^6H_{7/2}$  transfer. The use of  $Ba_2Ca(BO_3)_2 : Sm^{3+}$  ( $BC(BO) : Sm$ ) in combination with  $CaCO_3$  nanoparticles and yellow phosphor to form a conversion layer demonstrates the increase in red spectrum band of the generated white light. By varying the concentration of  $CaCO_3$  amount and maintain the  $BC(BO) : Sm$  concentration constant, the improvement in specific properties of WLED can be accomplished. According to the findings, the phosphor  $Ba_2Ca(BO_3)_2 : Sm^{3+}$  can prove utilizable via one near ultraviolet (n-UV) or blue chip for producing quality-enhanced WLEDs.

**Keywords:**  $Ba_2Ca(BO_3)_2 : Sm^{3+}$ ; X-ray diffraction;  $BO_3$  and  $BO_4$ ; Red spectrum; LEDs.

## 1. Introduction

Three-valence rare-earth (RE) incorporated samples have gained a lot of attention recently due to their implementations in illumination, thermic-luminescent (TL) dosage assessment, plasma exhibiting units, diodes emit white illumination (WLED) apparatuses as well as huge bar space, inexpensive price, and environmentally friendly qualities [1–3]. Samples incorporated using various RE elements may show radiation between the UV and near-infrared zones (NIZ) resulting from transformations between 4f and 4f or 4f and 5d [4–6] in order to meet the requirements for these uses. When it comes to producing bright orange-red illumination owing to 4f-4f transitions, the three-valence  $Sm^{3+}$  element featuring a 4f<sup>5</sup> structure would be one of the RE ions that is thought to be a key activator. Instead, the  $Sm^{3+}$  activated phos-

phors' stimulation peaks, which are at 345, 360, 375, 400, and 471 nm, are perfectly matched the InGaN chips' emitting maxima that generate NUV. As a result, the  $\text{Sm}^{3+}$  doped substances could be effortlessly stimulated by the commercially available chips, which is a crucial feature to remember when choosing an activator for phosphor substance. Due to their powerful  $^4G_{5/2} \rightarrow ^4H_{9/2}$  red emission, substances triggered using  $\text{Sm}^{3+}$  granules were also employed like red phosphors. It has been widely documented that  $\text{Sm}^{3+}$  ion activated substances have been employed because of the promising uses in WLEDs ( $\text{Ca}_3\text{Y}_2\text{Si}_3\text{O}_{12} : \text{Sm}^{3+}$ ,  $\text{Sr}_3\text{Bi}(\text{PO}_4)_3 : \text{Sm}^{3+}$ ,  $\text{Y}_2\text{Si}_4\text{N}_6\text{C} : \text{Sm}^{3+}$ ,  $\text{YAl}_3\text{B}_4\text{O}_{12} : \text{Sm}^{3+}$ ) and have the ability of covering the amber space with great effectiveness as well [7–10].

Owing to their huge band space and great heat steadiness, which are necessary before a phosphor to be taken into consideration for use in businesses, the alkaline orthoborates with the standardized formula  $\text{X}_2\text{Z}(\text{BO}_3)_2$  (X signifies Ba, Sr while Z signifies Ca, Mg) would be thought to be the most effective phosphors to the promising uses in solid state illumination. These phosphors have been documented for use in TL dosimetry and LED systems [11, 12].  $\text{Ba}_2\text{Ca}(\text{BO}_3)_2$ ,  $\text{Sr}_2\text{Mg}(\text{BO}_3)_2$ , and  $\text{Ba}_2\text{Mg}(\text{BO}_3)_2$  were reported to have monoclinic crystal structures with a space group of  $\text{C}2/m$  and a trigonal phase with a space group of  $\text{R}3m$ , respectively [13].  $\text{Ba}_2\text{Ca}(\text{BO}_3)_2$  as well as  $\text{Ba}_2\text{Mg}(\text{BO}_3)_2$  incorporated using  $\text{Tb}^{3+}$  were found to have luminous characteristics in 1974 [14]. It is believed that  $\text{Ba}_2\text{Ca}(\text{BO}_3)_2$  (short as  $\text{BC}(\text{BO})$ ) doped with RE ions is a very useful host for illumination studies due to their huge band gap, great stability, and coordination environment, which is the coordinating numeral for  $\text{Ba}^{2+}$  granules featuring nine O motes generating contorted polyhedron, being considered one dominating element in determining their morphological and optic characteristics, whereas  $\text{Ca}^{2+}$  granules featuring six O motes forming distorted octahedral with the existence of Borate hosts exhibit transparency to a broad spectrum of wavelengths, from ultra violet to infrared. A  $\text{Ce}^{3+}$  doped  $\text{BC}(\text{BO})$  featuring  $\text{Na}^+$  element acting in the form of one charge counter-

actor, for instance, was found to have good luminous characteristics in 2007 [15]. Following this, the luminous characteristics of  $\text{BC}(\text{BO}) : \text{Ce}^{3+}$ ,  $\text{Mn}^{2+}$  phosphors was reported with the generation of white illumination via altering the dosage for  $\text{Mn}^{2+}$  granules from  $\text{BC}(\text{BO}) : \text{Ce}^{2+}$  phosphors [16]. There have also been reports on the characteristics of near-ultraviolet-excited  $\text{BC}(\text{BO})$  featuring incorporated  $\text{Eu}^{3+}$  as well as  $\text{Tm}^{3+}$  [17, 18]. Yet no research has been done on the luminescence characteristics of  $\text{Sm}^{3+}$  ion doped  $\text{BC}(\text{BO})$ .

The goal of current researches were to develop novel phosphor materials that effectively close the amber gap. The  $\text{Ba}_2\text{Ca}(\text{BO}_3)_2 : \text{Sm}^{3+}$  phosphor can be a potential candidate to achieve this goal. The  $\text{Sm}^{3+}$ -doped  $\text{BC}(\text{BO})$  red phosphor here is produced using the solid-state reaction route. The red phosphor is mixed with the yellow phosphor and nanoparticle  $\text{CaCO}_3$  for modelling the white LED device. The luminescence properties of the as prepared phosphor and the modelled LED device are calculated and presented. The change in scattering particle  $\text{CaCO}_3$  is applied to the simulation process to monitor the performance of both colour quality and lumen output of the white LED. The simulation is carried out with Mie-scattering Monte Carlo theory and MATLAB computation. The obtained results show that addition of  $\text{Sm}^{3+}$ -doped  $\text{BC}(\text{BO})$  red phosphor broaden the emission band and induce the strength of red emission from the phosphor layer.

## 2. Experimental

### 2.1. Materials

By utilizing an elevated temperature solid state reaction technique, the  $\text{BC}(\text{BO}) : \text{Sm}^{3+}$  samples can be prepared. The initial chemical ingredients include  $\text{BaCO}_3$ ,  $\text{CaCO}_3$ ,  $\text{H}_3\text{BO}_3$ ,  $\text{Sm}_2\text{O}_3$ . All of them were used without further purification. According to previous studies with rare-earth-doped  $\text{BC}(\text{BO})$  phosphors, 2 mol% was the optimal dopants' concentration in the  $\text{BC}(\text{BO})$  host, yielding the greatest luminescence power for the phosphor [17, 19]. Thus, the amount of  $\text{Sm}^{3+}$  in the work was set at 2 mol%.

The typical synthesis of  $BC(BO):Sm^{3+}$  started with weighing the reactants based on the stoichiometric proportion and mixing them utilizing agate mortar and pestle for an hour. Subsequently, some ethyl alcohol was introduced into the mixture. The attained uniform combination was then transferred to an alumina pot for sintering under  $900\text{ }^\circ\text{C}$  within six hours. Finally, the products were cooled down to ambient heat level before being ground into powder. For determining the phase pureness as well as crystalline formation for individual  $Ba_2Ca(BO_3)_2$  as well as  $Ba_2Ca(BO_3)_2$  integrated with  $Sm^{3+}$ , power Xray diffraction (PXRD) assessment needs to be conducted with the profiles displayed within referential sources [20].

## 2.2. Characterizations

The luminescence excitation and emission spectra of the phosphor were collected with the Cary–Eclipse Spectrofluorometric apparatus featuring Xenon illumination under 150 watts in the form of one exciting means. Mie-scattering Monte Carlo simulation and MATLAB computation were utilized for simulating and examining the optical performance of the modelled WLED’s phosphor-conversion layer. The 3D model of a conventional package was built with the LightTool software, as shown in Figure 1.

## 3. Results and Discussion

### 3.1. Assessment of the BC(BO): Sm phosphor luminescence

When doping  $Sm^{3+}$  into the  $BC(BO)$  phosphor, the cation substitution is likely to occur between the  $Sm^{3+}$  and  $Ba^{2+}$  sites. It can be attributed to the difference percentages among their ionic radii ( $D_r$ ), which can be calculated using eq. 1:

$$D_r = \frac{R_1(\text{CN}) - R_2(\text{CN})}{R_1(\text{CN})} \times 100\% \quad (1)$$

where  $R_1(\text{CN})$  and  $R_2(\text{CN})$  represent the radii of  $Ba^{2+}$  and  $Sm^{3+}$ , respectively. The radius of  $Sm^{3+}$  and  $Ba^{2+}$  are  $1.12\text{ \AA}$  (CN = 8) and  $1.35\text{ \AA}$  (CN = 8), in turn; thus, the calculated

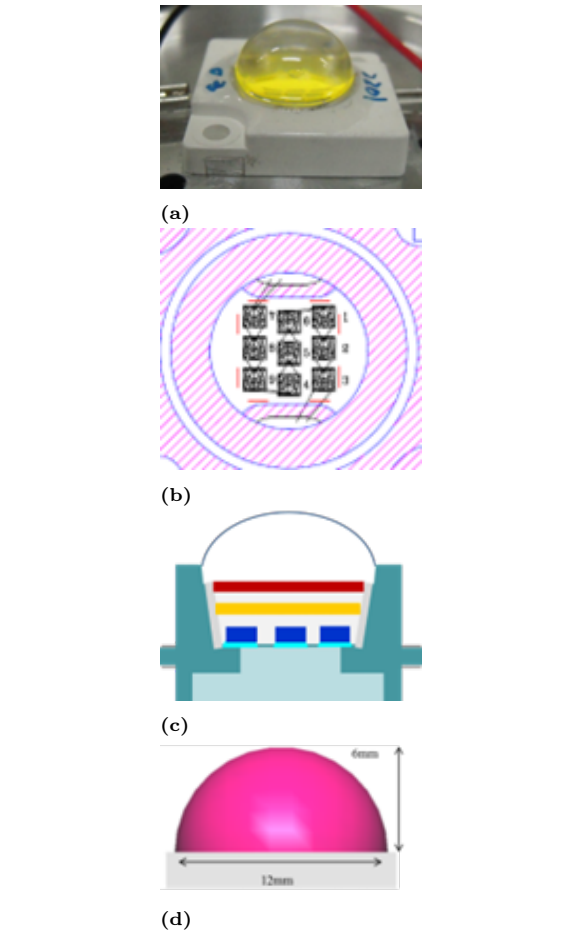
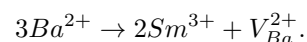


**Fig. 1:** WLED configuration: (a) WLED gadget, (b) Bonded chip setting, (c) WLED graphical depiction, (d) WLED recreation through LightTools.

$\Delta r$  is about 17%. It is advisable to have  $\Delta r$  smaller than 30%, in accordance with the Hume-Rothery rule [21], meaning that  $Sm^{3+}$  can replace the  $Ba^{2+}$ . When the  $Sm^{3+}$  enters the  $Ba^{2+}$  sites, a shrink in the lattice parameter can occur as the  $Sm^{3+}$  radius is smaller than that of  $Ba^{2+}$ . In the  $Ba_2Ca(BO_3)_2$  host, the  $Sm^{3+}$  inclusion can be primarily attributed to charge compensation mechanisms, leading to the formation of intrinsic defects within the material. The  $Sm^{3+}$  ions can occupy various positions, including substitutional sites of  $Ba^{2+}$  ions, interstitial sites, and  $V_{Ba}$  vacant sites. This process can be described by the equation:



The charge transmission bar (between  $O^{2-}$  and  $Sm^{3+}$ ) can induce the absorbing range at about 200–250 nm with regard to  $Sm^{3+}$ -doped  $BC(BO)$ . The other faint absorbing ranges from 350 nm to 500 nm are also found and are appropriate for the  $4f \rightarrow 4f$  transformations of the  $Sm^{3+}$  ion. The shifts between bottom states for  ${}^6H_{5/2}$  towards  ${}^6F_{11/2}$ ,  ${}^6F_{9/2}$ ,  ${}^6F_{7/2}$ , as well as  ${}^6F_{5/2}$  for  $Sm^{3+}$  granules can be attributed to the peaks in the range from 325 nm to 525 nm [22], with the most intense at about 402 nm ( ${}^6H_{5/2} \rightarrow {}^6L_{13/2}$ ).

Intersect alleviation (IA) procedures (non-radioactive power transmission) amid  $Sm^{3+}$  granules, being the outcome of an interchange interplay, radioactivity re-assimilation, or multipolar-multipolar interplay, are the main causes for dosage quenching. The critical distance ( $R_c$ ) among the nearby  $Sm^{3+}$  ions may be used to determine the type of contact mechanism. The power transmission's value of the critical range could become attainable via utilizing Blasse's formula in the following equation 2 [23, 24]:

$$R_c = 2 \left( \frac{3V}{4\pi X_c N} \right)^{1/3} \quad (2)$$

where  $X_c$  signifies the critical dosage for trigger granules and  $V$  signifies the capacity for a single cellule.  $Z$  signifies the cationic quantity within said cellule. Generally, the interchange interplay is rendered non-proficiently while merely one many-pole interactivity becomes effectual when the range among  $Sm^{3+}$  granules exceeds 5 Å. Nevertheless, the interchange interplay starts to work as said range becomes less than 5 Å.  $V = 303 \text{ \AA}^3$ ,  $Z = 2$ , while  $X_c$  reaches 0.02 in this instance, respectively. According to calculations, the critical power transfer range ( $R_c$ ) is 24.36 Å. The  $BC(BO) : Sm$  phosphor's  $R_c$  of  $Sm^{3+} - Sm^{3+}$  value is greater than 5 Å; therefore, the multipole-multipole interplay is the main working mechanism affecting concentration.

The illumination deterioration arches for  $BC(BO) : Sm^{3+}$  under various dosages for  $Sm^{3+}$  stimulated under 402 nm while tracked under 601 nm discharges. Equation 3 may be utilized to fit the deterioration curves featuring

the opening-sequence exponential deterioration expression:

$$I(t) = I_0 + A \exp \left( -\frac{t}{\tau} \right) \quad (3)$$

$I$  and  $I_0$  signify the luminous intensities at time  $t$  and  $t = 0$ , respectively, and  $A$  signifies fitting constants.  $t$  also represents the passage of temporal units, and  $\tau$  shows the deterioration durations. The  $BC(BO) : Sm^{3+}$ 's identified deterioration lifespans for the deterioration curve and Equation 3 are 0.1191, 0.1101, 0.1079, 0.1012, and 0.0996 ms, which illustrates how the decay lifetime decreases as the dosage of  $Sm^{3+}$  ions increases.

One of the most critical considerations when assessing the effectiveness of phosphors is thought to be the color purity. The hue purity for  $BC(BO) : Sm^{3+}$  is measured by utilizing expression 4:

$$Color \ purity = \frac{\sqrt{(x - x_n)^2 + (y - y_n)^2}}{\sqrt{(x_i - x_n)^2 + (y_i - y_n)^2}} \times 100 \quad (4)$$

$(x_i, y_i)$  signifies the coordinating numeral for the illuminant spot,  $(x_s, y_s)$  signifies the coordinating numeral for the specimen point, whereas  $(x_d, y_d)$  signifies the CIE coordinating numeral for the corresponding dominant wavelength at 601 nm.

In this instance, choosing (0.596, 0.403), (0.642, 0.357), as well as (0.3333, 0.3333) in the case of  $(x_s, y_s)$ ,  $(x_d, y_d)$ , as well as  $(x_i, y_i)$  coordinates respectively, yields the chroma clarity for samples. The hue pureness for  $Ba_2Ca(BO_3)_2 : Sm^{3+}$  reaches 82.29% using these coordinates.

The McCamy empirical formula in Equation 5 identifies the hue correlated heat level (CCT) in the case of  $Ba_2Ca(BO_3)_2 : Sm^{3+}$ :

$$CCT = -473n^3 + 3601n^2 - 6861n + 5514.32 \quad (5)$$

$n$  equates to  $(x - x_e)/(y - y_e)$ , whereas the focal point of chromaticity would be located under  $x_e = 0.3320$  and  $y_e = 0.1858$ . With the CCT figure being below 5000 K, warm white illumination utilized in household gadgets manifests; whereas with said figure being above 5000 K, cool white illumination utilized in business lighting manifests. For LEDs in solid-state illumination, the red phosphor  $Ba_2CaBO_3)_2 : Sm^{3+}$

may therefore become employed in the form of a suitable orange-red sample [25–27].

### 3.2. Influence from $\text{CaCO}_3$ @red upon WLED proficiency

The  $BC(BO) : \text{Sm}^{3+}$  phosphor's photoluminescence excitation (PLE) spectral factor was captured under one emitting wavelength reaching 601 nm. Strong wide-scope and thin-line absorbing ranges make up the excitation spectrum. The  $\text{O}^{2-} \rightarrow \text{Sm}^{3+}$  transition charge transfer is thought to be the cause of the powerful absorbing range of 200–250 nm that is centered at 205 nm (CT). The low-power absorbing ranges at 344 nm ( ${}^6\text{H}_{5/2} \rightarrow {}^4\text{H}_{9/2}$ ), 360 nm ( ${}^6\text{H}_{5/2} \rightarrow {}^4\text{D}_{3/2}$ ), 375 nm ( ${}^6\text{H}_{5/2} \rightarrow {}^6\text{P}_{7/2}$ ), 402 nm ( ${}^6\text{H}_{5/2} \rightarrow {}^4\text{L}_{13/2}$ ), as well as 471 nm ( ${}^6\text{H}_{5/2} \rightarrow {}^4\text{L}_{13/2}$ ) are caused by  $\text{Sm}^{3+}$  transitions from  $4f \rightarrow 4f$ . The  ${}^6\text{H}_{5/2} \rightarrow {}^6\text{L}_{13/2}$  transition state is represented by the intense stimulation maximum at 402 nm, which is one of the  $4f \rightarrow 4f$  transitions.

With 402 nm stimulation, the PL emitting spectrum of  $BC(BO) : 0.02\text{Sm}^{3+}$  phosphor is noted, and it includes highest points placed at 565 nm, 601 nm, 649 nm, and 711 nm. These peaks are ascribed to the  $\text{Sm}^{3+}$  ion's transformation states  ${}^4\text{G}_{5/2} \rightarrow {}^6\text{H}_{5/2}$ ,  ${}^4\text{G}_{5/2} \rightarrow {}^6\text{H}_{7/2}$ ,  ${}^4\text{G}_{5/2} \rightarrow {}^6\text{H}_{9/2}$ , and  ${}^4\text{G}_{5/2} \rightarrow {}^6\text{H}_{11/2}$ , in turn. Said sample exhibits a bright orange-red radiation under 601 nm, which is associated with the  ${}^4\text{G}_{5/2} \rightarrow {}^6\text{H}_{7/2}$  transformation [28]. The emission of  $BC(BO) : \text{Sm}^{3+}$  appears under 601 nm with the stimulation wavelength reaching 402 nm. Said mechanism is a good fit for n-UV-based LEDs' wavelength. The findings demonstrate the effectiveness of this substance as an orange-red sample in LED apparatuses subject to solid-state illumination.

Figure 2 displays the emitting spectra of the  $\text{CaCO}_3@BC(BO) : \text{Sm}$ -based WLED. The complete range of white emission highlights the power of phosphor for augmenting orange-red as well as blue illumination. It is possible to modify  $\text{CaCO}_3$  characteristics, subsequently modifying the profile for illumination dispersal as well as absorptivity, thus improving illumina-

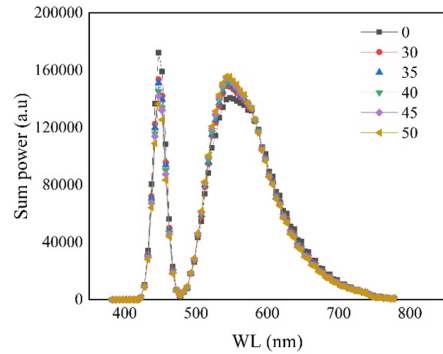


**Fig. 2:** Luminescent energy for WLED subject to different  $BC(BO):\text{Sm}$  dosages

tion efficiency. The prominent peaks at blue (450 nm) and bright red ( $\sim 600$  nm) are also demonstrated, indicating the efficiency of using  $BC(BO) : \text{Sm}^{3+}$  phosphor to increase the red spectral energy. Besides, upon the addition of higher  $\text{CaCO}_3$  in the phosphor film, the peaks' intensities change notably. The blue peak declines, and the red peak becomes more intense, which indicates that the blue light used by the phosphor increases and the conversion of phosphor is promoted. Such results can be attributed to the higher scattering performance by  $\text{CaCO}_3$  nanoparticles.

The interaction among the illumination discharge dispersal element as well as  $\text{CaCO}_3$  presence in the  $BC(BO) : \text{Sm}^{3+}$  film is shown in Figure 3. As can be seen, the scattering coefficient shows a perceptible increase under greater phosphor concentrations, signifying an increase in illumination scattering. It is possible to enhance wavelength conversion and light transmission efficiency while also increasing the ratio of  $\text{CaCO}_3$ . Brightness can be increased by causing onward blue illumination discharge dispersal to rise as well as blue illumination dispersal along with re-absorptivity to be lessened. This is done by raising the amount of  $\text{CaCO}_3$  while decreasing the amount of yellow phosphor  $YGA : \text{Ce}$  and keeping the  $BC(BO) : \text{Sm}^{3+}$  amount fixed. As a result, the variation in the related color temperature (CCT) is likewise decreased. Figure 4 demonstrates that the concentration of  $YGA : \text{Ce}$  drops when  $\text{CaCO}_3$  concentration increases, in contrast to Figures 5 and 6, which exhibit CCT being constant with dosage. Under

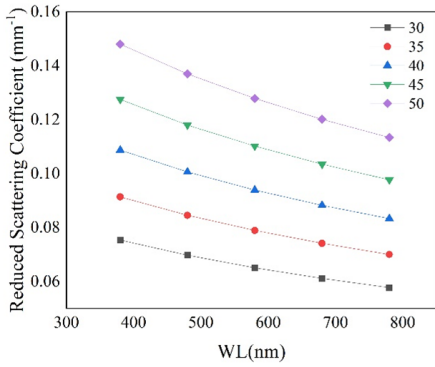


Fig. 3: Scattering coefficients with different  $BC(BO)$  :  $Sm$  proportions

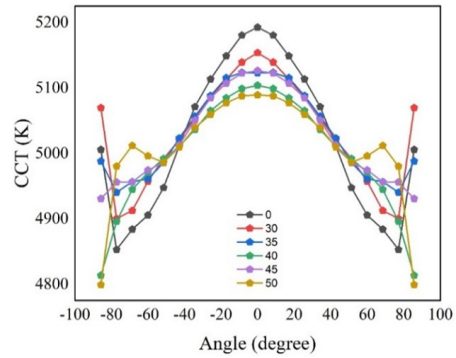


Fig. 5: CCT values with different  $BC(BO)$  :  $Sm$  proportions

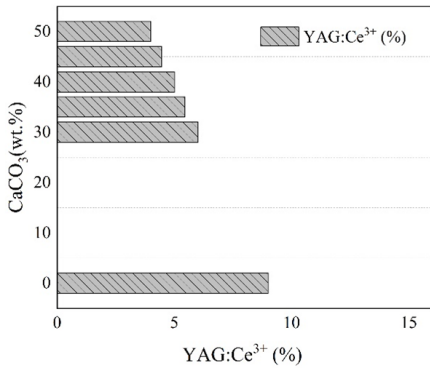


Fig. 4: YGA:Ce phosphor proportion values with different  $BC(BO)$  :  $Sm$  proportions

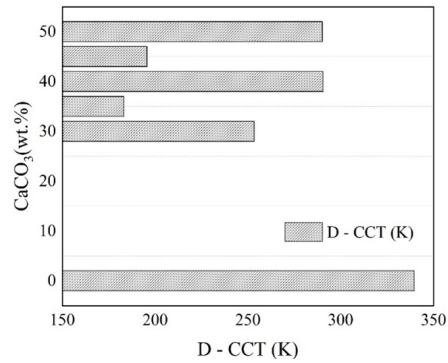


Fig. 6: Hue variation values with different  $BC(BO)$  :  $Sm$  proportions

supplementary administration of  $CaCO_3$ , the phosphor layer will become effective at diminishing the disparity in the layer's CCT, as shown in Figure 5. Under roughly 900 K, the  $\Delta CCT$  eventually achieves a nadir outcome under 35%  $CaCO_3$ , see Figure 6, which is about 150 K beneath the outcome with no  $CaCO_3$  percentages being employed.

The increase in  $CaCO_3$  amount can induce the brightness of the white light emission, as seen in Figure 7. As can be observed, the best results were acquired via 50% of  $CaCO_3$  concentration whilst the most undesirable ones occurred via 0 - 30%  $CaCO_3$ . Resulting from greater rear reflection as well as re-absorptivity, said mechanism yields a fainted blue discharge as well as an inconsistent chroma allocation. Greater  $CaCO_3$  proportions could encourage optic alteration among blue as well as yellow or

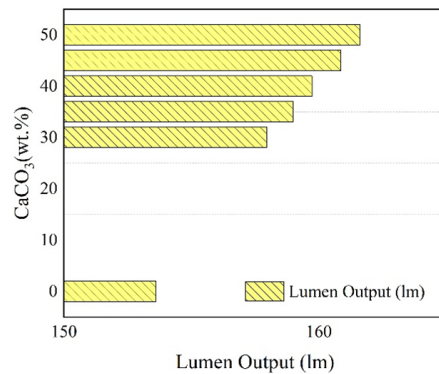
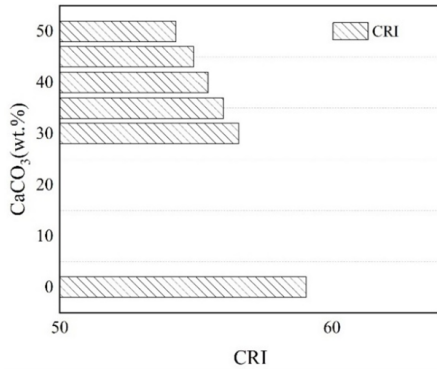
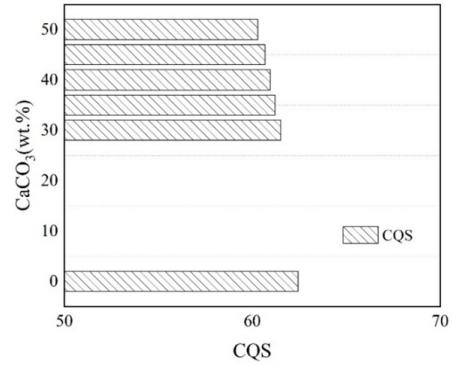


Fig. 7: Luminescence strength with different  $BC(BO)$  :  $Sm$  proportions



**Fig. 8:** CRI for WLED subject to different  $BC(BO) : Sm$  proportions



**Fig. 9:** CQS values with different  $BC(BO) : Sm$  dosages

orange-red as the concerned sample absorbs additional blue rear-reflected illumination. Once reaching a sufficient  $CaCO_3$  concentration, the phosphor coating begins to expand. The converted light's emission spectrum may become limited, resulting from every reflection from various surfaces. In other words, greater phosphor presence would increase the quantity for transmuted illumination subject to rear reflection, reducing luminous intensity while increasing CCT. In this case, the decrease of phosphor concentration obtained by increasing  $CaCO_3$  amount can help to address the issue. With the simulated WLED, it was discovered that a ratio of 50%  $CaCO_3$  worked well to boost brightness, yet the color homogeneity is not significantly improved with the same  $CaCO_3$  amount. However, attempts to aim for a greater concentration are not advised as it is known that excessive phosphor concentrations can lead to several undesirable outcomes, including higher scattering, lower illumination proficiency, color alterations as well as thermic problems [29–31]. The light level as well as chroma rendering for WLEDs prove strongly dependent on the concentration for  $CaCO_3$ . When  $CaCO_3$  concentration increased to 50%, color rendition values were assessed using the chromatic rendition criterion (CRI) as well as chromatic performance scope (CQS), which revealed one steady reduction, as shown in Figures 8 and 9, respectively. Unbalanced blue, green, and yellow-orange hues are potential reasons for the apparent reductions in CRI and CQS. The high  $CaCO_3$  dose causes more dispersion, as already mentioned, and the

chroma in illumination discharges tends to tilt to the zone of yellow-orange, creating an unbalance. This phosphor needs additional study on other properties, like the particle size, which our research study will analyze to control the CRI and CQS [32, 33].

## 4. Conclusion

In conclusion, this study explored the formation as well as luminescence attributes in  $Ba_2Ca(BO_3)_2 : Sm^{3+}$  samples made via the standard solid-state approach. Luminescence measurements of the red phosphor and phosphor-conversion sheet for white light-emitting diodes were performed using Mie-scattering Monte Carlo simulation and MATLAB computation. The phosphor exhibited one wide discharge spectrum featuring one prominent peak under roughly 601 nm subject to 402 nm exciting process, attributed to the  $Sm^{3+}$  ion's  $^4G_{5/2} \rightarrow ^6H_{7/2}$  transition. Utilizing  $Ba_2Ca(BO_3)_2$  in conjunction with  $CaCO_3$  nanoparticles and yellow phosphor to form a conversion layer enhanced the red spectral band of the emitted white light. By varying the concentration of  $CaCO_3$  while maintaining a constant concentration of  $Ba_2Ca(BO_3)_2$ , improvements in the specific properties of WLEDs were achieved. The results indicate that the  $Ba_2Ca(BO_3)_2$  phosphor can be effectively used with an n-UV or blue chip to produce high-quality WLEDs.

## References

- [1] M. H. N. Thi, N. T. P. Loan, and N. D. Q. Anh. Study of red-emitting LaAsO<sub>4</sub> : Eu<sup>3+</sup>+ phosphor for color rendering index improvement of WLEDs with dual-layer remote phosphor geometry. *Telecommun. Comput. Electron. Control.*, 18(6):3210, 2020.
- [2] H. T. Tung, N. D. Q. Anh, and H. Y. Lee. Impact of phosphor granule magnitudes as well as mass proportions on the luminous hue efficiency of a coated white light-emitting diode and one green phosphor film. *Optoelectron. Adv. Mater. - Rapid Commun.*, 18:58–65, 2024.
- [3] N. D. Q. Anh. Nano scattering particle: an approach to improve quality of the commercial led. *The Univ. Danang - J. Sci. Technol.*, 22(3):53–57, 2024.
- [4] Q. Dai, C. E. Duty, and M. Z. Hu. Semiconductor-nanocrystals-based white light-emitting diodes. *Small*, 6(15):1577–1588, 2006.
- [5] H. Fujii, H. Sakurai, N. K. Tani, N. L. Mao, K. Wakisaka, and T. Hirao. Vivid-red and highly efficient phosphors bearing diphenylquinoxaline units and their application to organic light-emitting devices. *Int. Meet. for Future Electron Devices*, pages 35–36, 2024.
- [6] W. T. Hong, J. H. Lee, H. I. Jang, S. J. Park, J. S. Joo, and H. K. Yang. Orange-red light emitting europium doped calcium molybdate phosphor prepared by high energy ball milling method. *20th Microoptics Conf. (MOC)*, 365:1–2, 2015.
- [7] R. Li, H. Li, Y. Peng, H. Cheng, Z. Chen, and M. Chen. Development of rgb phosphor-in-glass for ultraviolet-excited white light-emitting diodes packaging. *17th Int. Conf. on Electron. Packag. Technol. (ICEPT)*, pages 94–97, 2016.
- [8] J.E. Murphy, W. Beers, M. Butts, S.J. Camardello, A. Chowdhury, and W. Cohen. Narrow band emitting led phosphors for wide color gamut displays & energy efficient ssl. *IEEE Photonics Conf. (IPC)*, 46:1, 2018.
- [9] Y. Peng, H. Cheng, Z. Chen, M. Chen, and R. Li. Multi-layered red, green, and blue phosphor-in-glass for ultraviolet-excited white light-emitting diodes packaging. *17th Int. Conf. on Electron. Packag. Technol. (ICEPT)*, 5:61–64, 2016.
- [10] M. Saito and H. Kondo. Battery-independent emergency illumination with rgb phosphors. *Proc. 39th Annu. 2005 Int. Carnahan Conf. on Secur. Technol.*, pages 222–225, 2005.
- [11] C. Shao, Z. Peng, B. Yu, Z. Li, and X. Ding. The detail study on the effect of the flow during the curing process of phosphor particles on the color performance. *21st Int. Conf. on Electron. Packag. Technol. (ICEPT)*, pages 1–4, 2020.
- [12] C.-Y. Shen, K. Li, Q.-L. Hou, H.-J. Feng, and X.-Y. Dong. White LED based on YAG: CE,GD phosphor and CDSE-ZNS core/shell quantum dots. *IEEE Photonics Technol. Lett.*, 12:884–886, 2010.
- [13] C. Shen, C. Zhong, K. Li, and J. Ming. High color rendering index WLED based on YAG:Ce phosphor and Cds/Zns core/shell quantum dots. *Photonics Optoelectron. Meet. (POEM) 2009: Optoelectron. Devices Integr.*, page 751609, 2009.
- [14] J.K. Sheu, S.J. Chang, C.H. Kuo, Y.K. Su, L.W. Wu, and Y.C. Lin. White-light emission from near UV InGaN-GaN LED chip precoated with blue/green/red phosphors. *IEEE Photonics Technol. Lett.*, 15:18–20, 2003.
- [15] H.-K. Shih, C.-N. Liu, W.-C. Cheng, and W.-H. Cheng. Phosphor-in-glass for high performance WLEDs by reduction phosphor interaction and AR coating. *IEEE Photonics Technol. Lett.*, 33(20):1143–1146, 2021.
- [16] C. Guo, L. Luan, Y. Xu, F. Gao, and L. Liang. White light-generation phosphor Ba<sub>2</sub>Ca(BO<sub>3</sub>)<sub>2</sub>:Ce<sup>3+</sup>,

- Mn<sup>[sup 2+]</sup> for light-emitting diodes. *J. Electrochem. Soc.*, 155(11):J310, 2008.
- [17] L. Liu, Y. Zhang, J. Hao, C. Li, Q. Tang, C. Zhang, and Q. Su. Thermoluminescence characteristics of terbium-doped Ba<sub>2</sub>Ca(BO<sub>3</sub>)<sub>2</sub> phosphor. *Phys. Status Solidi (A)*, 202(14):2800–2806, 2005.
- [18] S. Jayakiruba, S. S. Chandrasekaran, P. Murugan, and N. Lakshminarasimhan. Excitation-dependent local symmetry reversal in single host lattice Ba<sub>2</sub>A(BO<sub>3</sub>)<sub>2</sub>:Eu<sup>3+</sup> [A = Mg and Ca] phosphors with tunable emission colours. *Phys. Chem. Chem. Phys.*, 19(26):17383–17395.
- [19] M.-Y. Ma, W.R. Song, and C.Y. Ji. Luminescence properties of tunable red-green emitting phosphor Ba<sub>2</sub>Ca(BO<sub>3</sub>)<sub>2</sub>:Eu<sup>3+</sup>, Tb<sup>3+</sup>. *Optoelectron. Lett.*, 13(2):131–134, 2017.
- [20] M. Manhas, V. Kumar, V. K. Singh, J. Sharma, R. Prakash, V. Sharma, A.K. Bedyal, and H.C. Swart. A novel orange-red emitting Ba<sub>2</sub>Ca(BO<sub>3</sub>)<sub>2</sub>:Sm<sup>3+</sup> phosphor to fill the amber gap in LEDs: Synthesis, structural and luminescence characterizations. *Curr. Appl. Phys.*, 17(11):1369–1375, 2017.
- [21] P. Shao, P. Xiong, Y. Xiao, Z. Chen, D. Chen, and Z. Yang. Self-recoverable NIR mechanoluminescence from Cr<sup>3+</sup> doped perovskite type aluminate. *Adv. Powder Mater.*, 3(2):100165, 2023.
- [22] M. Huang, X. Yang, and F. Jiang. Dielectric and luminescent properties of Sm<sup>3+</sup> doped Ba(Zn<sub>1/3</sub>Nb<sub>2/3</sub>)O<sub>3</sub> ceramics with perovskite structure. *Mater. Res. Express*, 5(6):066301, 2018.
- [23] S.-H. Yang, S.-M. Liao, and C.-H. Wang. Enhancement on luminescence of ZnAl<sub>2</sub>O<sub>4</sub>:Eu<sup>3+</sup> phosphor with carbon dots addition. *8th Int. Conf. on Appl. Syst. Innov. (ICASI)*, page 166–169, 2022.
- [24] C.-C. Tsai. Thermal aging performance analyses of high color rendering index of glass-based phosphor-converted white-light-emitting diode. *IEEE Trans. on Device Mater. Reliab.*, 15(4):617–620, 2015.
- [25] T. P. Vo and N. D. Q. Anh. Effect of Y<sub>2</sub>O<sub>3</sub>:Eu<sup>3+</sup> phosphor powder size on the performance of white LED lamp. *5th Int. Symp. on Next-Generation Electron. (ISNE)*, 2016.
- [26] W.-L. Wang, J. K. Moore, A. C. Martiny, and F. W. Primeau. Convergent estimates of marine nitrogen fixation. *Nature*, 566(7743):205–211, 2019.
- [27] A. Herrmann, D. Friedrich, T. Zschechel, and C. Rüssel. Luminescence properties of sm<sup>3+</sup> doped alkali/earth alkali orthoborates of the type XZBO<sub>3</sub> with X = Li, Na, Cs and Z = Ca, Sr, Ba. *J. Lumin.*, 214:116550, 2019.
- [28] M.-J. Chen, V. T. Le, D. Q. A. Nguyen, and T. C. Tran. ZNO nanoparticles in bettering the color uniformity of phosphor-converted white LED lights. *J. Adv. Eng. Comput.*, 4(3):173, 2020.
- [29] H.-Y. Lee, P. X. Le, and D. Q. A. Nguyen. The impacts of red-emitting mg<sup>2+</sup>ti<sup>4+</sup>:mn<sup>4+</sup> phosphor on color quality of dual-layer remote phosphor configuration. *J. Adv. Eng. Comput.*, 3(3):464, 2019.
- [30] V. T. Pham, N. H. Phan, G.-F. Luo, H.-Y. Lee, and D. Q. A. Nguyen. The application of calcium carbonate CaCO<sub>3</sub> and titania TiO<sub>2</sub> for color homogeneity and luminous flux enhancement in PC-LEDs. *J. Adv. Eng. Comput.*, 5(2):75, 2021.
- [31] N.-Z. Zhuo, N. Zhang, Y.-H. Chen, P. Jiang, S.-W. Cheng, and Y.-H. Zhu. Fabrication and optical properties of white LED based on laminated remote phosphor film. *15th China Int. Forum on Solid State Light. Int. Forum on Wide Bandgap Semicond. China (SSLChina: IFWS)*, pages 1–4, 2018.
- [32] M. Zheng, W. Ding, F. Yun, D. Xia, Y. Huang, and Y. Zhao. Study of high cri white light-emitting diode devices with

multi-chromatic phosphor. *IEEE 64th Electron. Components Technol. Conf. (ECTC)*, pages 2236–2240, 2014.

- [33] P. H. Yuen, H. H. Shiung, and M. Devarajan. Influence of phosphor packaging configurations on the optical performance of chip on board phosphor converted warm white LEDs. *Fifth Asia Symp. on Qual. Electron. Des. (ASQED 2013)*, 27:329–333, 2013.

## About Authors

**Nguyen Thi Phuong THAO** was born in Quang Ngai City, Vietnam in 1983. She received the M.Ss. degree in Electrical Engineering from Ho Chi Minh University of Technology, Ho Chi Minh City, Vietnam in 2008, and received the

Ph.D. degree in Electrical Engineering from VSB-Technical University of Ostrava, Czech Republic, in 2022. Presently, She is working as a lecturer at the Faculty of Electrical and Electronics Engineering, Ton Duc Thang University, Ho Chi Minh City, Vietnam. Her research interests involve optics science. She can be contacted at email: nguyenthiphuongthao@tdtu.edu.vn.

**Hsiao-Yi LEE** was born in Hsinchu city, Taiwan. He has been working at the Department of Electrical Engineering, National Kaohsiung University of Science and Technology, Kaohsiung, Taiwan. His research interest is optics science. He can be contacted at email: leehy@nkust.edu.tw.